

Case Study

Cryo-EM and SPR Analysis of SARS-CoV-2 Spike Protein Neutralization by Cayman Antibody Complex

Zahra Assar[†], Kendall Muzzarelli[†], Ieva Drulyte[§], Bill Ho[†], Judy Hines[†], Jeremy Bickel[†], Mazdak Radjainia[§], and Michael Pisano[†]
Cayman Chemical[†], Thermo Fisher Scientific[§]

Overview

- Cayman Chemical has made a SARS-CoV-2 (human) neutralizing recombinant antibody which disrupts the S1 RBD-ACE2 interaction.
- Surface plasmon resonance (SPR) was used to evaluate the recombinant neutralizing antibody's ability to block binding of SARS-CoV-2 S1 receptor-binding domain (RBD) variants to human angiotensin-converting enzyme 2 (hACE2).
- Cryo-electron microscopy (cryo-EM) single-particle analysis was used to determine the structure of intrinsically difficult-to-crystallize, >0.5 MDa SARS-CoV-2 spike:Fab complex.
- This case study shows the structure and conformational analysis of the SARS-CoV-2 spike glycoprotein trimer in complex with a Fab derived from a recombinant SARS-CoV-2 neutralizing antibody. Cayman's engineered recombinant antibody could effectively block the interaction of hACE2 with S1 RBD wild-type and Alpha variants better than that with the Beta variant.
- These structural results from cryo-EM and SPR studies could aid in the development of vaccines and therapeutics for the SARS-CoV-2 variants.

Background

SARS-CoV-2 is an enveloped positive-stranded RNA virus, a member of the *Betacoronavirus* genus and the causative agent of COVID-19. As of September 2021, the number of COVID-19 cases worldwide had reached over 223 million. In addition, the number of deaths from COVID-19 exceeds 4.3 million. SARS-CoV-2 infection can result in the production of neutralizing antibodies (nAbs), which bind to the SARS-CoV-2 spike RBD preventing further viral entry and infection, starting approximately 4-10 days after symptom onset.^{1,2}

Experimental Need

Understanding the structural motif and binding mode of this neutralizing antibody response could benefit vaccine design and drug discovery by revealing the features that contribute to an effective antibody response. This is particularly salient considering the emerging SARS-CoV-2 variants that have potential to escape immunity endowed by established vaccine or antibody treatments. In collaboration with Thermo Fisher Scientific, we utilized both cryo-EM and SPR to determine the structure of SARS-CoV-2 spike glycoprotein in complex with the nAb fragment antigen-binding (Fab) regions and characterize the molecular interactions, respectively.

Antibody Development and Fab Preparation

Cayman developed a [SARS-CoV-2 \(human\) Neutralizing Recombinant Antibody \(Item No. 32526\)](#) that recognizes the SARS-CoV-2 spike glycoprotein and disrupts the RBD interaction with the ACE2 receptor that SARS-CoV-2 uses to enter host cells. This antibody contains an immunoglobulin G heavy-chain variable region 3-53 common to most neutralizing antibodies that target the RBD of the spike protein and bears a single point mutation.³ The Fab fragment was generated for structural studies using a Pierce™ Fab Preparation Kit.

Cryo-EM Sample Preparation, Data Collection, and Processing

SARS-CoV-2 hexaprotline spike protein ectodomain was mixed with the Fab fragment at 1.4 molar ratio and incubated for five minutes.⁴ Right before plunge freezing, 0.005 or 0.02% (w/v) fluorinated octyl maltoside (FOM) was added to the sample to overcome the preferred orientation. Spike-Fab sample was applied to glow-discharged (20 mAmp, 30 sec, Quorum GloQube®) Quantifoil® R1.2/1.3 grids, blotted for five seconds using blot force 2 and plunged frozen into liquid ethane using Vitrobot Mark IV (Thermo Fisher Scientific) (**Figure 1A**). The data were collected on a Thermo Scientific Krios G4 Cryo-Transmission Electron Microscope (Cryo-TEM) equipped with Selectris X Imaging Filter (Thermo Fisher Scientific) and Falcon 4 Direct Electron Detector camera (Thermo Fisher Scientific) operated in electron-event representation (EER) mode.

Data processing was performed in Relion-3 and cryoSPARC™ single particle analysis suites.^{5,6} After motion and CTF correction, 716,690 particles were picked from 4,048 micrographs from two separate data collections (2,475 images with 0.005% FOM and 1,573 images with 0.02% FOM). After 2D classification (**Figure 1B**) and heterogenous refinement, the best particle stack consisting of 100,618 particles was subjected to non-uniform refinement with C3 symmetry imposed yielding a map with 2.85 Å global resolution (**Figure 1C-F**).⁷ Following global refinement, a mask was made encompassing one RBD with the Fab bound (**Figure 2A**). Particles were imported in Relion and symmetry expanded for focused classification. Following two rounds of focused classification (**Figure 2D,E**), the best particle stack consisting of 144,483 particles was imported back to cryoSPARC™ and refined using local refinement yielding a 5.15 Å map (**Figure 2B,C,F**). The local map was masked and sharpened using DeepEMhancer tool.⁸ Data acquisition and analysis parameters can be found in **Table 1**.

The cryo-EM map revealed an S trimer with three Fabs bound to open RBDs. Despite relatively high global resolution (2.85 Å), due to flexibility, the RBD-Fab region was resolved to lower resolution and could only be visible at a low threshold level (**Figure 1D**). We used focused classification in Relion followed by local refinement in cryoSPARC™ to obtain a ~5 Å map of the region corresponding to the Fab variable domain and RBD, which markedly improved local resolution due to conformational dynamics relative to the rest of the S trimer.

Table 1. Parameters used for cryo-EM data acquisition and analysis.

Data Acquisition and Processing Parameters	
Grid	Quantifoil® R1.2/1.3
Camera	Selectris X-Falcon 4
Slit width (eV)	10
Nominal magnification	130,000x
Pixel size (Å)	0.96
Dose rate (e-/pix/sec)	8.04
Exposure time (sec)	5.82
Total dose (e-/Å ²)	51.5
Fractionation	EER
Autofocus	After centering
Hole centering	AFIS (6 µm image shift)
Number of images	4,048
Throughput	~220/hour
Total number of particles picked	716,690
Particles in the final reconstruction	100,618

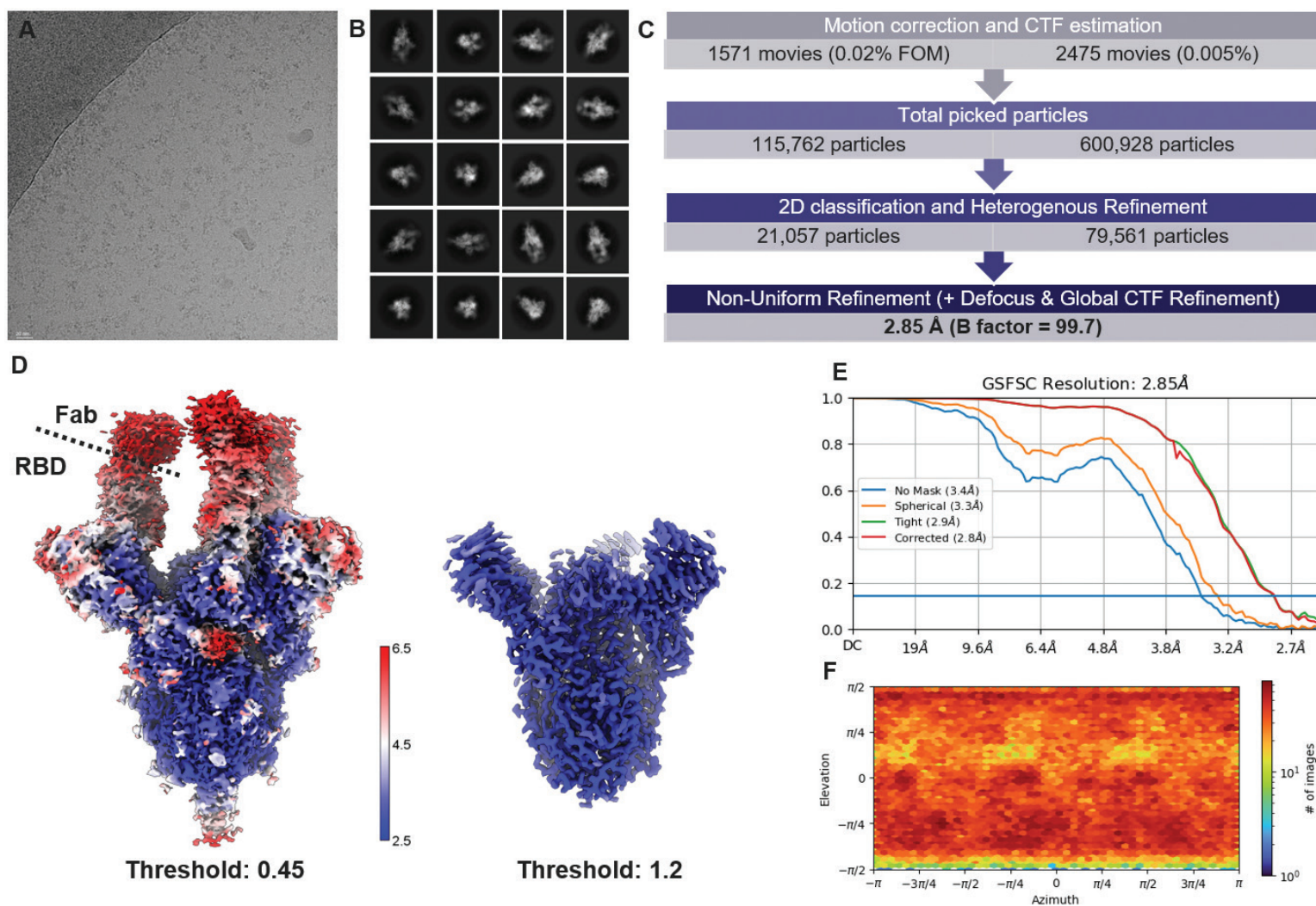


Figure 1. Cryo-EM single particle analysis of 6P-stabilized SARS-CoV-2 pre-fusion spike ectodomain in complex with a Fab.⁴ **A.** Representative cryo-EM micrograph. **B.** 2D class averages. **C.** Workflow and metrics. **D.** 3D reconstruction of the SARS-CoV-2 spike ectodomain in complex with a Fab colored according to local resolution. RBDs with the bound Fabs are in an open conformation and only visible at a lower threshold level. **E.** Gold-standard Fourier Shell Correlation curve. **F.** Angular distribution plot.

Structure Refinement and Interpretation

To characterize the structural properties favorable for RBD recognition, we characterized the interface between the Fab CDR loops and SARS-CoV-2 spike RBD.

Crystal structures of RBD (6M0J.pdb) and CC12.3 Fab (6XC7.pdb) were rigid body fit into the local cryo-EM map using UCSF Chimera.⁹ Coot and Phenix were used to further refine the SARS-CoV-2 spike protein/nAb (Fab) complex to characterize the interface between the two proteins.^{10,11} The RBD-Fab model revealed the binding interface at a molecular detail. This information can be used to guide the rational engineering of SARS-CoV-2 neutralizing antibodies (**Figure 2**).

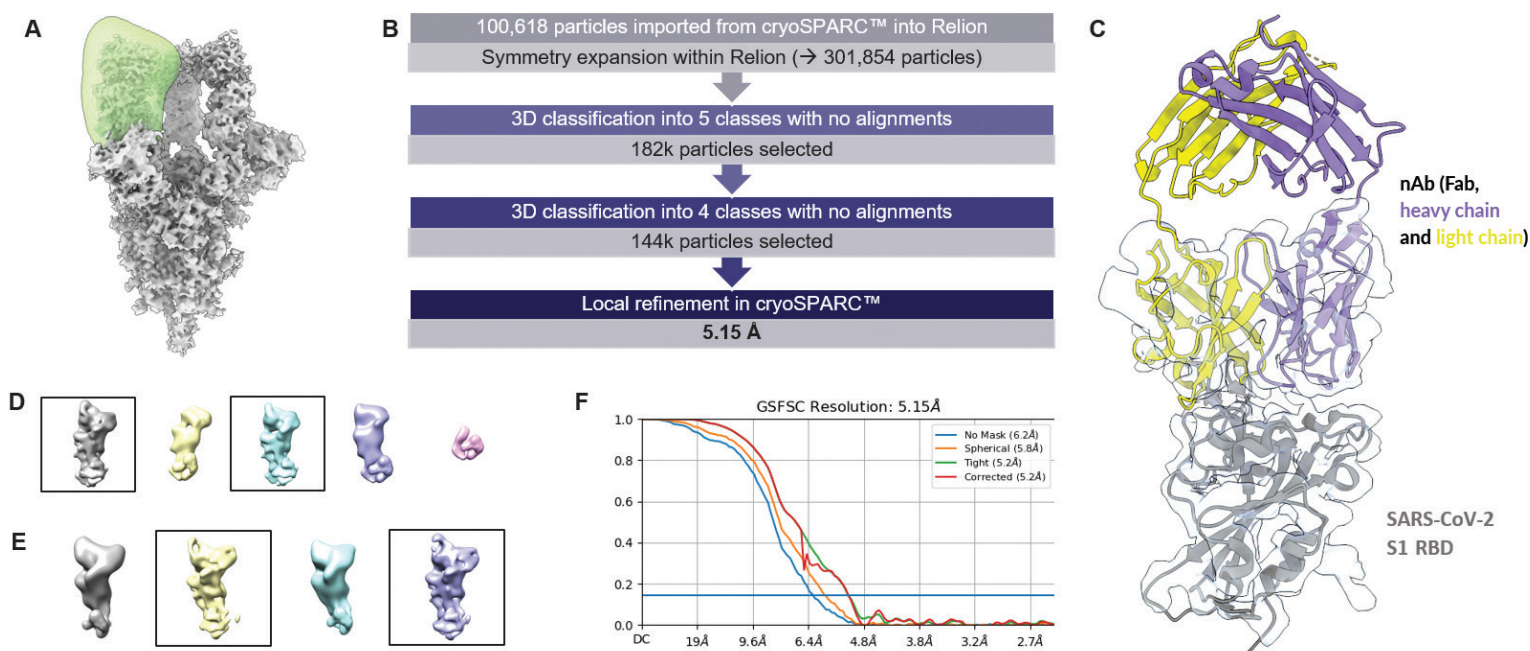


Figure 2. Localized refinement of the RBD-Fab region. **A.** Localized mask (green) surrounding RBD-Fab monomer. **B.** Workflow and metrics. **C.** Local refinement map showing Fab (light and heavy chains are colored yellow and purple, respectively) and the SARS-CoV-2 RBD (grey) with the corresponding region of cryo-EM density (transparent grey surface). **D.** Results from the first round of focused classification in Relion. Particles from boxed classes were selected for further processing. **E.** Results from the second focused classification. Particles from boxed classes were selected for local refinement in cryoSPARC™. **F.** Gold-standard Fourier Shell Correlation curve.

SPR Studies

SPR using a Biacore instrument was performed to understand the molecular interactions and binding mechanism of this nAb. We established a competition assay between SARS-CoV-2 nAb (Fab) and ACE2 against S1 RBD and determined whether the nAb had reduced neutralizing capabilities towards the variants versus wild-type (WT) using SPR. For these experiments, S1 RBD WT (**Item No. 30590**), Alpha (**Item No. 33867**), and Beta (**Item No. 33868**) variants as well as hACE2 (**Item No. 30587**) proteins made using Cayman's established mammalian expression system were used.

Multi-cycle kinetics (MCK) competition assays were performed to look at the nAb's ability to neutralize SARS-CoV-2 S1 RBD WT and variants when ACE2 is added at K_D , $4x K_D$, and $\frac{1}{4} K_D$ (10 nM ACE2 data is shown in **Figure 3**). Overall, data correlated well with single-cycle kinetics (data not shown), and the nAb provided better blocking against ACE2 binding.

Based on the results of the competition assay (fixed concentration of ACE2), the nAb (Fab) provided better blocking against ACE2 binding with WT and Alpha variants ($IC_{50}s = 64$ and 68 nM, respectively) compared to the Beta variant ($IC_{50} = 120$ nM). The same results were obtained using *in vitro* and cell-based assays.

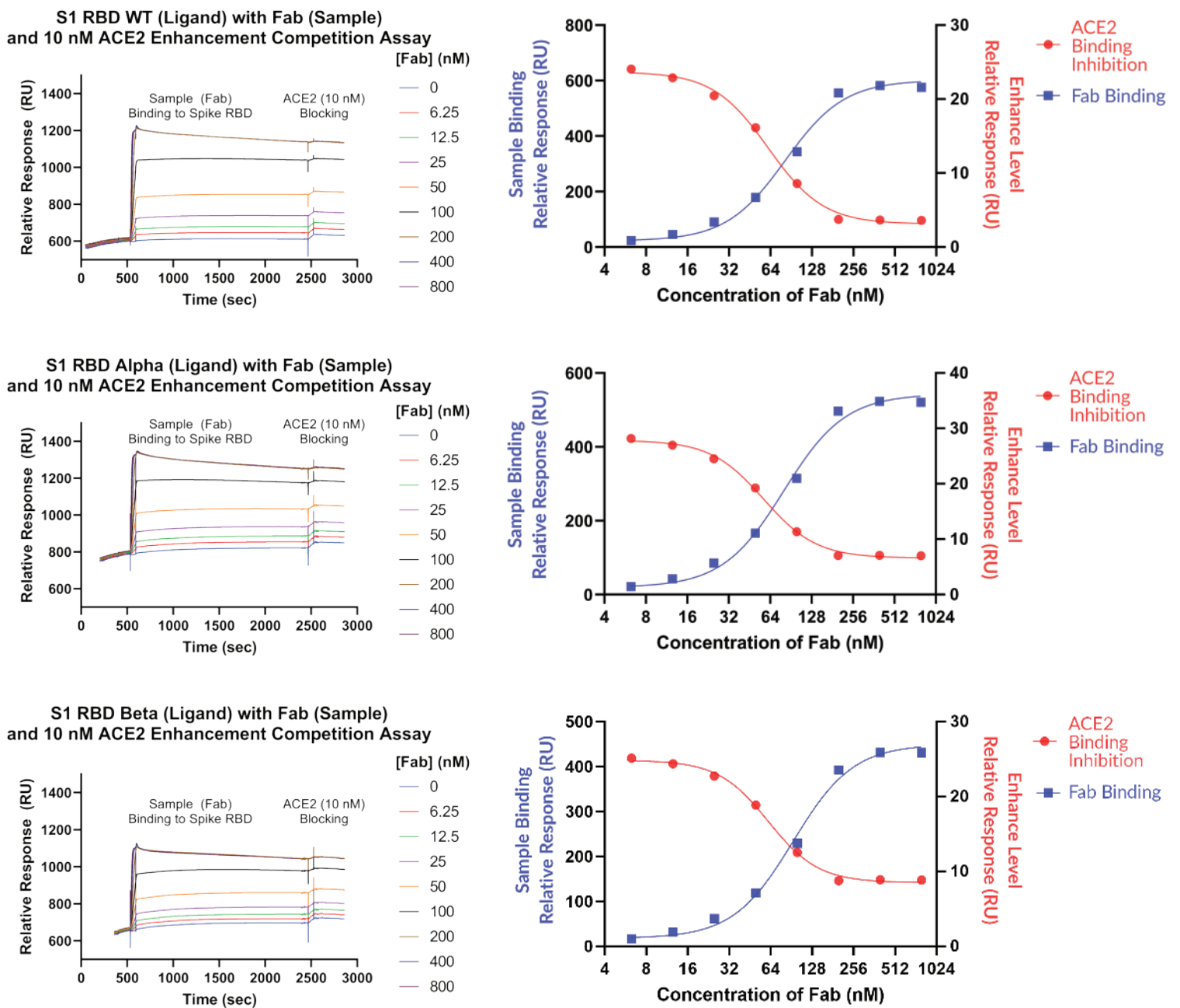


Figure 3. SPR data and MCK competition assays for SARS-CoV-2 nAb (Fab) and ACE2 with S1 RBD WT and variants.

Summary

Both cryo-EM and SPR techniques provided structural and functional insights into SARS-CoV-2 neutralizing recombinant antibody blocking the spike RBD-ACE2 interaction. In this study, the cryo-EM structure of the SARS-CoV-2 Spike/nAb (Fab) complex was determined in collaboration with Thermo Fisher Scientific. Based on the structure of this complex, we could characterize the binding of Cayman's recombinant neutralizing antibody to the S1 RBD in the presence of hACE2, which revealed a strong affinity for the WT and Alpha variants over the Beta variant. Knowledge of these structural data will help further the design of more potent and selective recombinant antibodies towards the new variants of the virus.

Visit www.caymanchem.com/structuralbiology to discover Cayman's **Structure-Based Drug Design Services**. Our team of experts is made up of medicinal and computational chemists, protein scientists, and structural biologists with proven experience to advance the drug discovery and development efforts of our clients. **Contact us** for help with your next discovery.

Visit www.thermofisher.com/PharmaceuticalResearch to learn more about Cryo-EM for Pharmaceutical Research.

Author Contribution

Cryo-EM analysis was performed by Ieva Drulyte at Thermo Fisher Scientific.

References

1. Wang, Y., Zhang, L., Sang, L., *et al.* Kinetics of viral load and antibody response in relation to COVID-19 severity. *J. Clin. Invest.* **130(10)**, 5235-5244 (2020).
2. Xiang, F., Wang, X., He, X., *et al.* Antibody detection and dynamic characteristics in patients with coronavirus disease 2019. *Clin. Infect. Dis.* **71(8)**, 1930-1934 (2020).
3. Yuan, M., Liu, H., Wu, N.C., *et al.* Structural basis of a shared antibody response to SARS-CoV-2. *Science* **369(6507)**, 1119-1123 (2020).
4. Hsieh, C.-L., Goldsmith, J.A., Schaub, J.M., *et al.* Structure-based design of prefusion-stabilized SARS-CoV-2 spikes. *Science* **369(6510)**, 1501-1505 (2020).
5. Zivanov, J., Nakane, T., Forsberg, B.O., *et al.* New tools for automated high-resolution cryo-EM structure determination in RELION-3. *Elife* **7**, e42166 (2018).
6. Punjani, A., Rubinstein, J.L., Fleet, D.J., *et al.* cryoSPARC: Algorithms for rapid unsupervised cryo-EM structure determination. *Nat. Methods* **14(3)**, 290-296 (2017).
7. Punjani, A., Zhang, H., and Fleet, D.J. Non-uniform refinement: Adaptive regularization improves single-particle cryo-EM reconstruction. *Nat. Methods* **17(12)**, 1214-1221 (2020).
8. Sanchez-Garcia, R., Gomez-Blanco, J., Cuervo, A., *et al.* DeepEMhancer: A deep learning solution for cryo-EM volume post-processing. *Commun. Biol.* **4(1)**, 874 (2021).
9. Pettersen, E.F., Goddard, T.D., Huang, C.C., *et al.* UCSF Chimera—a visualization system for exploratory research and analysis. *J. Comput. Chem.* **25(13)**, 1605-1612 (2004).
10. Emsley, P., Lohkamp, B., Scott, W.G., *et al.* Features and development of Coot. *Acta Crystallogr. D Biol. Crystallogr.* **66(Pt 4)**, 486-501 (2010).
11. Liebschner, D., Afonine, P.V., Baker, M.L., *et al.* Macromolecular structure determination using X-rays, neutrons and electrons: Recent developments in Phenix. *Acta Crystallogr. D Struct. Biol.* **75(Pt 10)**, 861-877 (2019).

